

Structural, electrochemical and photophysical investigations of Re(I)-complexes of κ^3N -tridentate heterocyclic ligands

Amlan K. Pal and Garry S. Hanan*

Département de Chimie, Université de Montréal, 2900 Edouard-Montpetit, Montréal, Québec H3T-1J4, Canada

Supporting Information

Materials, methods and instrumentation

Nuclear magnetic resonance (NMR) spectra were recorded in CD₃CN, CDCl₃, and DMSO-d₆ at room temperature (r.t.) on a Bruker AV400 (400 MHz) spectrometer for ¹H NMR and at 100 for ¹³C NMR, respectively. Chemical shifts are reported in part per million (ppm) relative to residual solvent protons (1.94 ppm for CD₃CN, 7.26 ppm for CDCl₃, 2.50 ppm for DMSO-d₆) and the carbon resonance (1.24 ppm for CD₃CN, 77.00 ppm for CDCl₃, 39.43 ppm for DMSO-d₆) of the solvent.

All the photophysical measurements were carried out in deaerated acetonitrile at r.t. in septa-sealed quartz cells. Absorption spectra were measured on a Cary 500i UV-Vis-NIR Spectrophotometer. For luminescence spectra a Cary Eclipse Fluorescence spectrofluorimeter was used. Electrochemical measurements were carried out in argon-purged purified acetonitrile at room temperature with a BAS CV50W multipurpose potentiostat. The working electrode was a glassy carbon electrode. The counter electrode was a Pt wire, and the pseudo-reference electrode was a silver wire. The reference was set using an internal 1 mM ferrocene/ferrocinium sample at 395 mV vs. SCE in acetonitrile. The concentration of the compounds was about 1 mM. Tetrabutylammonium hexafluorophosphate (TBAP) was used as supporting electrolyte and its concentration was 0.10 M. Cyclic voltammograms of **L1**, **L2**, **1** and **2** were obtained at scan rates of 50, 50, 10 and 25 mVs⁻¹, respectively. The criteria for reversibility were the separation of 60 mV between cathodic and anodic peaks, the close to unity ratio of the intensities of the cathodic and anodic currents, and the constancy of the peak potential on changing scan rate. Differential pulse voltammetry was conducted with a sweep rate of 20 mVs⁻¹ and a pulse amplitude, width and period of 50 mV, 50 ms and 200 ms, respectively.

Experimental uncertainties are as follows: absorption maxima, ± 2 nm; molar absorption coefficient, 10%; redox potentials, ± 10 mV, emission maxima, ± 2 nm.

1,3,4,6,7,8-Hexahydro-2H-pyrimido[1,2-(a)]pyrimidine (**H-hpp**), 2,6-dibromopyridine, 2,6-dichloropyrazine, (\pm) BINAP, *t*-BuOK were purchased from Aldrich and used as received. $\text{Re}_2(\text{CO})_{10}$, $\text{Pd}(\text{OAc})_2$ were purchased from Pressure Chemicals. Ligand **L1** was synthesized using literature procedure.¹

Synthesis of **L2**:

(\pm) BINAP (0.09 mmol, 60 mg) was placed in an oven-dried, nitrogen-purged round-bottomed flask that was sealed with a septum. Dry toluene (3 mL) was added via syringe. The resulting suspension was heated at 90 °C for 2 min to dissolve the BINAP. This was cooled to room temperature and $\text{Pd}(\text{OAc})_2$ (0.06 mmol, 14 mg) was added and stirred for 3 min. To the resulting bright yellow solution, 2,6-dichloropyrazine (3.2 mmol, 479 mg) and 1,3,4,6,7,8-hexahydro-2*H*-pyrimido[1,2-*a*]pyrimidine (6.9 mmol, 962 mg) were added. Stirring for 5 min at ambient temperature resulted in a pale orange slurry to which was added *t*-BuOK (9.0 mmol, 1.01 g). The reaction mixture was then stirred at 90 °C for 16 h, was cooled to room temperature and diethyl ether (60 mL) was added and the mixture was filtered. Evaporation of the filtrate followed by purification by column chromatography on deactivated alumina using 3:2 (DCM:MeOH, v/v) afforded the ligand (**L2**) as crystalline pale yellow solid. Yield = 736 mg (65 %). ¹H NMR (DMSO-d₆, 400 MHz); 8.38 (s, 2 H), 3.70 (t, $J^t = 6$ Hz, 4 H), 3.25 (t, $J^t = 6$ Hz, 4 H), 3.19 (t, $J^t = 6$ Hz, 4 H), 3.15 (t, $J^t = 6$ Hz, 4 H), 1.94 (quint., $J^{qt} = 6$ Hz, 4 H), 1.77 (quint., $J^{qt} = 6$ Hz, 4 H) ppm. ¹³C NMR (DMSO-d₆, 100 MHz); 149.6, 147.9, 130.7, 47.9, 47.6, 43.1, 42.5, 22.8, 22.1 ppm. HRMS (ESI), m/z: 355.23526 [M+H]⁺ ($\text{C}_{18}\text{H}_{27}\text{N}_8$ requires 355.23532; Δppm -0.17),

178.12134 [M+2H]²⁺ ($C_{18}H_{28}N_8$ requires 178.12130; Δppm 0.23). Anal. Calc. for $C_{18}H_{26}N_8$: C, 60.99; H, 7.39; N, 31.61. Found: C, 60.99; H, 7.42; N, 31.58.

[$Re(\text{L1})(CO)_3][Br]$ (**1**):

$Re(CO)_5Br$ (50 mg, 0.123 mmol) was dissolved in hot dry toluene (30 mL) under a N_2 atmosphere. After cooling to ambient temperature, **L1** (48 mg, 0.136 mmol) was added to the resulting colourless solution. The suspension was heated at 80 °C for 3 h under a N_2 atmosphere in the dark. A colourless precipitate was observed upon completion of the reaction. The precipitate was isolated by filtration, washed with toluene (3x40 mL) and dried under vacuum to afford complex **1** as a pale yellow solid. Crystals suitable for X-ray crystallography were grown by diffusion of diethyl ether into a concentrated solution of **1** in chloroform:acetone (1:3, v/v). Yield = 80 mg (93%). ¹H NMR ($CDCl_3$, 400 MHz); 8.12 (t, J^t = 8 Hz, 1 H), 7.34 (d, J^d = 8 Hz, 2 H), 4.10 (d, J^d = 12 Hz, 2 H), 3.64 (m, 4 H), 3.52 (m, 2 H), 3.44 (m, 4 H), 3.37 (m, 2 H), 2.47 (m, 2 H) 2.32 (m, 2 H), 2.01 (m, 4 H), 1.65 (d, J^d = 12 Hz, 2 H). ¹³C NMR ($CDCl_3$, 100 MHz); 196.1, 154.2, 153.1, 143.4, 110.7, 51.6, 48.7, 46.5, 22.4, 21.6 ppm (one of the six different methylene carbons could not be seen), ¹³C NMR (CD_3CN , 100 MHz); 197.4, 155.3, 154.3, 143.4, 111.0, 52.3, 49.3, 49.2, 47.1, 22.7, 22.2 ppm (although one of the methylene carbons could not be seen in $CDCl_3$ solvent, it could be seen when recorded in CD_3CN). HRMS (ESI), m/z: 624.17347 [M-Br]⁺ ($C_{22}H_{27}N_7O_3^{187}Re$ requires 624.17274; Δppm 1.17). Anal. Calc. for $C_{22}H_{27}N_7O_3ReBr$: C, 37.55; H, 3.87; N, 13.93. Found: C, 37.54; H, 3.78; N, 13.82.

[$Re(\text{L2})(CO)_3][Br]$ (**2**):

$Re(CO)_5Br$ (50 mg, 0.123 mmol) was dissolved in hot dry toluene (30 mL) under a N_2 atmosphere. After cooling to ambient temperature, **L2** (48 mg, 0.135 mmol) was added to the

resulting colourless solution. The suspension was heated at 80 °C for 6 h under a N₂ atmosphere in the dark. An olive-green precipitate was observed upon completion of the reaction time. The precipitate was isolated by filtration, washed with toluene (2x10 mL) and Et₂O (2x10 mL) and dried under vacuum to afford complex **2** as a olive-green solid. Long needle shaped crystals suitable for X-ray cryatallography could be grown by diffusion of diethyl ether into a concentrated solution of **2** in dichloromethane. Yield = 78 mg (91%). ¹H NMR (CD₃CN, 400 MHz); 8.42 (s, 2 H), 4.13 (dt, J^{dt} = 14, 4 Hz, 2 H), 3.67 (m, 4 H), 3.41 (m, 8 H), 3.28 (ddd, J^{ddd} = 12, 10, 6 Hz, 2 H), 2.25 (m, 4 H), 1.98 (d, J^d = 6 Hz, 2 H) 1.90 (m, 2H). ¹³C NMR (CD₃CN, 100 MHz); 197.2, 154.4, 150.4, 132.8, 53.2, 49.9, 49.8, 47.3, 23.4, 22.3 ppm. HRMS (ESI), m/z: 625.16817 [M-Br]⁺ (C₂₁H₂₆N₈O₃¹⁸⁷Re requires 625.16799; Δppm 0.29). Anal. Calc. for C₂₁H₂₆N₈O₃ReBr: C, 35.80; H, 3.72; N, 15.90. Found: C, 35.81; H, 3.69; N, 15.77.

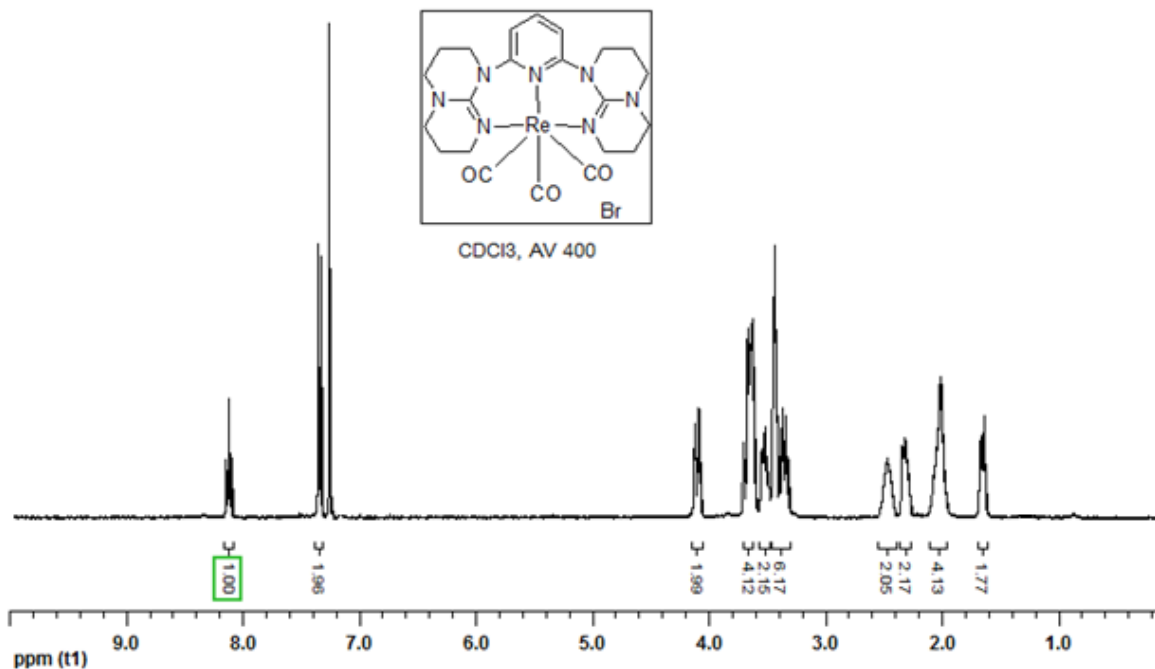


Figure S1. ¹H NMR spectrum of **1** in CDCl₃ at 400 MHz at room temperature.

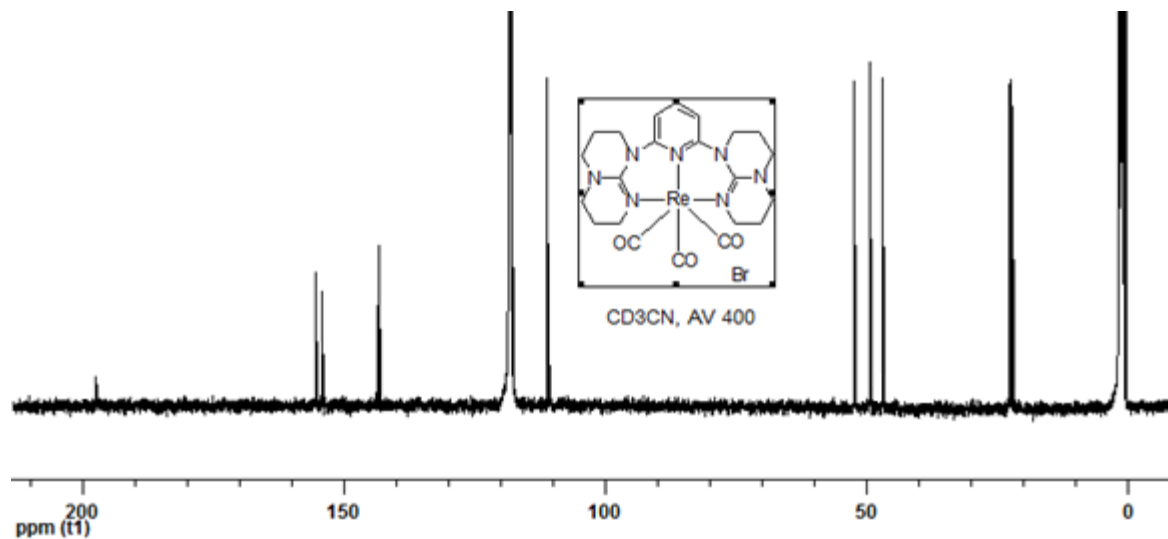


Figure S2. ^{13}C NMR spectrum of **1** in CD_3CN at 400 MHz at room temperature.

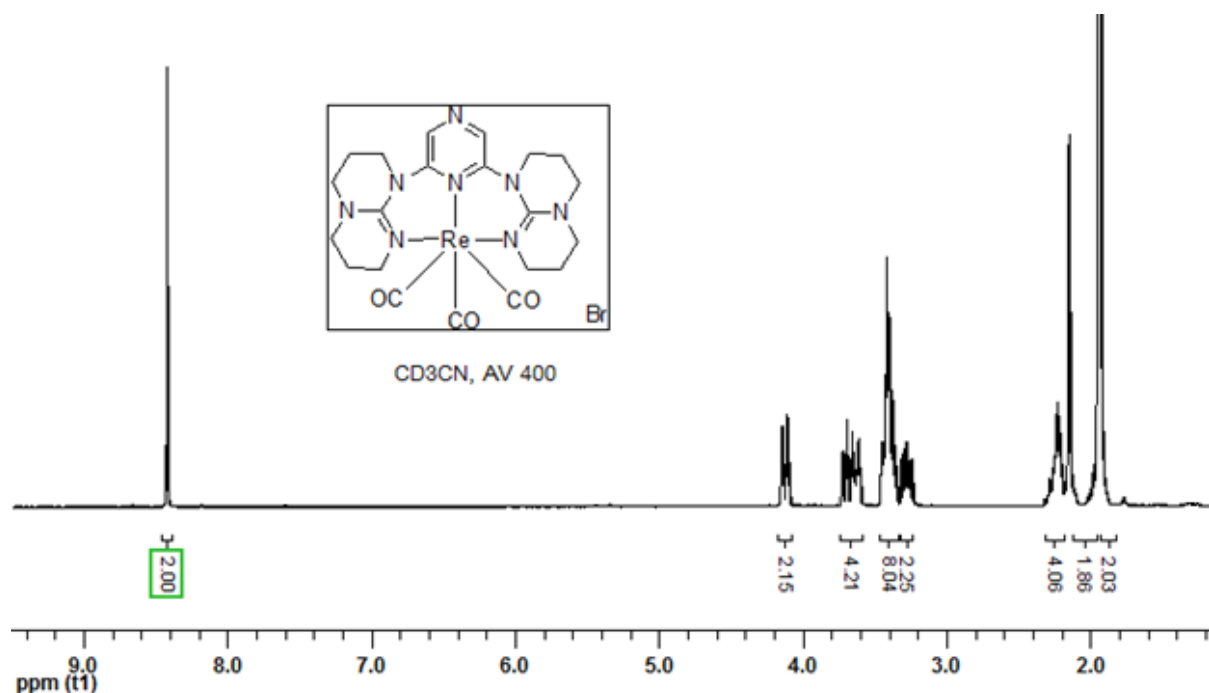


Figure S3. ^1H NMR spectrum of **2** in CD_3CN at 400 MHz at room temperature.

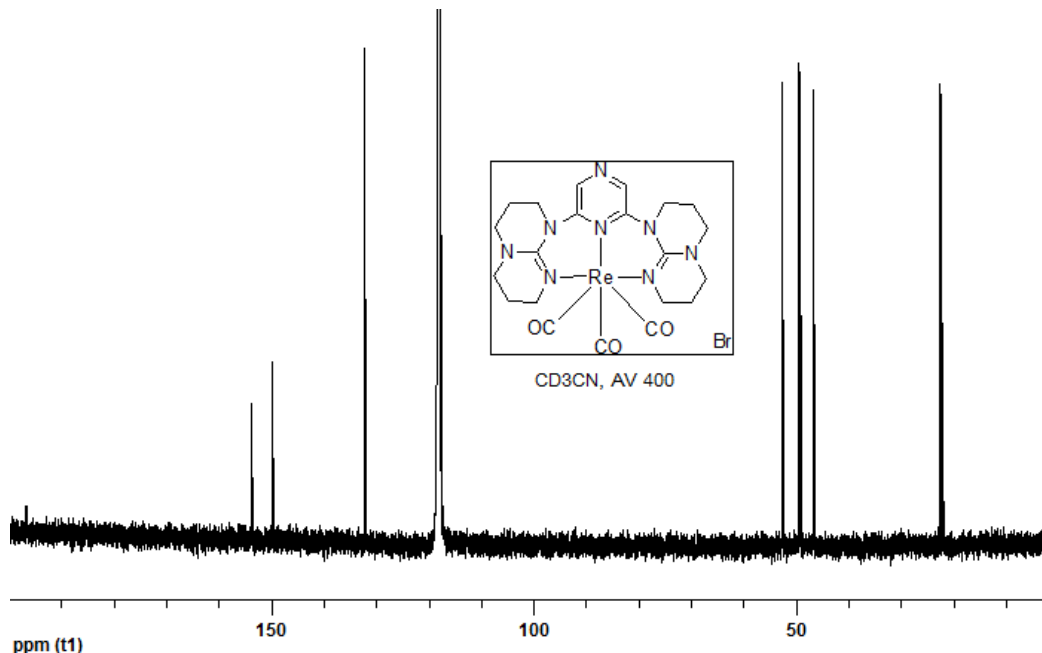


Figure S4. ^{13}C NMR spectrum of **2** in CD_3CN at 400 MHz at room temperature.

X-ray diffraction studies:

Diffraction data were collected on a Bruker SMART 6000 with Montel 200 monochromator, equipped with a rotating anode source for Cu K α radiation. The diffraction quality of the crystals were checked, revealing in some cases poor diffraction with a large amount of diffuse scattering, signaling extensive crystal disorder. Cell refinement and data reduction were done using APEX2.² Absorption corrections were applied using SADABS.³ Structures were solved by direct methods using SHELXS97 and refined on F^2 by full-matrix least squares using SHELXL97.⁴ All non-hydrogen atoms were refined anisotropically. Hydrogen atoms were refined isotropic on calculated positions using a riding model. For compound **1** the highest difference peak is 0.93 Å far from Re-atom and the deepest hole is 0.73 Å from Re-atom. In addition, in **1** four more peaks with density around 1 e/Å³ were present essentially due to the quality of the crystal employed, which was the best available. For compound **2** the highest difference peak is 1.01 Å far from

atom C9 and is believed due to positional disorder of this atom. This disorder was not taken into account for modelling. Except this Q-peak, four other Q-peaks of electron density ranging from 2.25-1.16 e/Å³ were located and they are in close proximity (1.37-1.05 Å) to the Re-atom.

Table S1. Crystallographic data for complexes **1** and **2**.

Compound	1	2
CCDC Number	922649	975057
Formula	[C ₂₂ H ₂₇ N ₇ O ₃ Re][Br]	[C ₂₁ H ₂₆ N ₈ O ₃ Re][Br]
Mw (g/mol); d _{calcd.} (g/cm ³)	703.62; 1.981	704.61; 2.002
T (K); F(000)	150(2); 684	150(2); 684
Crystal System	Triclinic	Triclinic
Space Group	P-1	P-1
Unit Cell: a (Å)	8.1289(3)	8.2315(6)
b (Å)	11.6833(5)	11.7681(6)
c (Å)	13.8021(6)	13.3936(8)
α (°)	105.115(2)	104.882(3)
β (°)	105.785(2)	105.407(3)
γ (°)	99.199(1)	99.732(3)
V (Å ³); Z	1179.57(8); 2	1168.99(13); 2
θ range (°); completeness	3.51-69.18; 0.981	3.61-69.34; 0.984
R _{fl} :collec./indep.; R _{int}	70414/4350; 0.0490	45519/4333; 0.0536
μ (mm ⁻¹)	12.397	12.524
R1(F); wR(F ²); GoF(F ²) ^a	0.0271; 0.0709; 1.104	0.0337; 0.0907; 1.082
Residual electron density	1.528; -0.935	2.646; -1.040

^aR1(F) based on observed reflections with I>4σ(I) for **1** and **2**; wR(F²) and GoF(F²) based on all data for all compounds.

Table S2. Comparison of bond distances and angles in **1** and **2**.

Compound	Bond Length			Angle		
		Obs. (X-ray)	Calc. (DFT)		Obs. (X-ray)	Calc. (DFT)
1	Re1-N1	2.175(3)	2.21295	N1-Re1-N4	78.14(11)	78.048
	Re1-N4	2.199(3)	2.24161	N1-Re1-N7	78.75(11)	78.049
	Re1-N7	2.183(3)	2.24161	N4-Re1-N7	88.41(11)	89.895
	Re1-C21	1.901(5)	1.92552			
	Re1-C20	1.922(4)	1.92647			
	Re1-C22	1.933(4)	1.92647			
	O2-C21	1.170(6)	1.16266			
	O1-C20	1.144(6)	1.16305			
	O3-C22	1.153(5)	1.16305			
2	Re1-N1	2.163(4)	2.19737	N1-Re1-N5	77.95(15)	77.893
	Re1-N8	2.194(4)	2.24680	N1-Re1-N8	78.61(14)	78.298
	Re1-N5	2.195(4)	2.25059	N5-Re1-N8	89.05(15)	91.413
	Re1-C19	1.934(6)	1.92749			
	Re1-C20	1.931(5)	1.92935			
	Re1-C21	1.900(6)	1.92698			
	O1-C19	1.135(7)	1.16226			
	O2-C20	1.140(7)	1.16149			
	O3-C21	1.184(7)	1.16254			

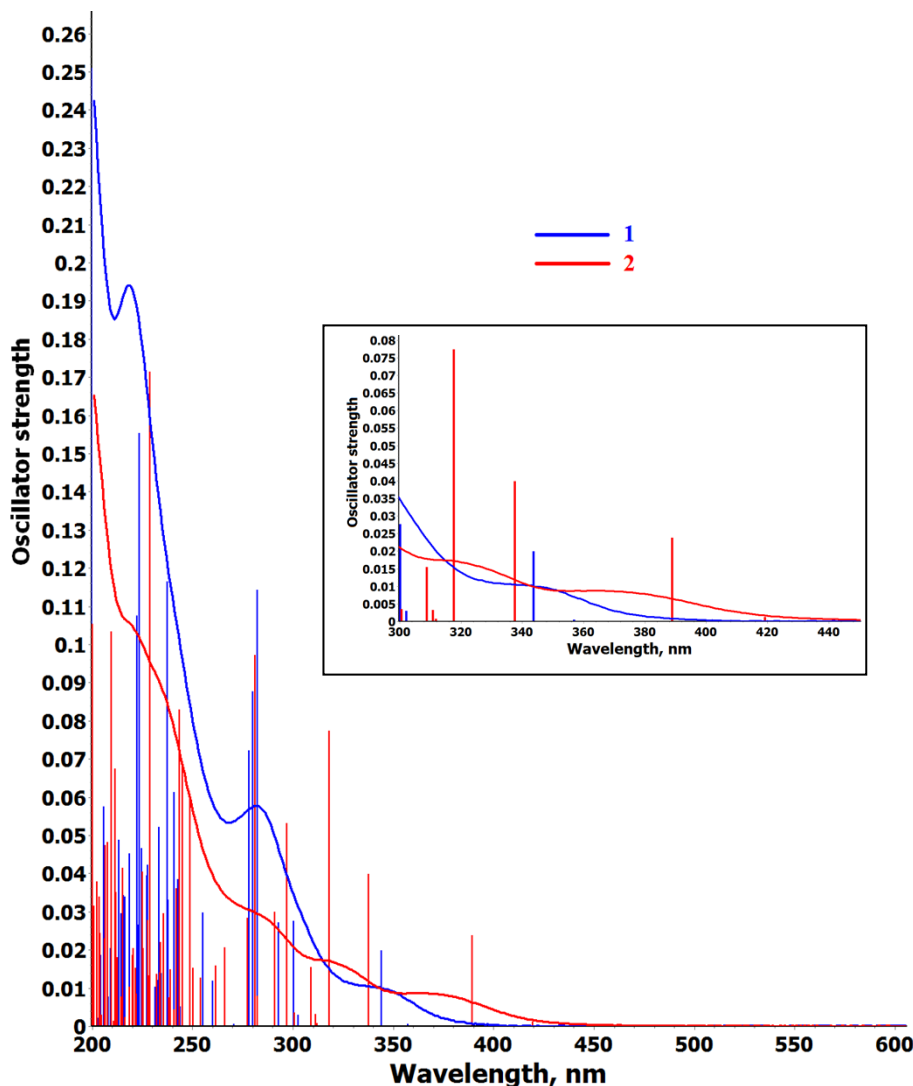


Figure S5. Overlay of experimental (curved lines) absorption spectra and calculated (straight lines) oscillator strengths at different wavelengths of **1** (blue) and **2** (red), at ambient temperature in dry acetonitrile.

Table S3. UV-vis and emission data of **L1**, **L2**, **1** and **2**.

Compound	UV-vis ^a λ_{max} , nm ($\epsilon \times 10^3$, M ⁻¹ cm ⁻¹)				Emission ^a λ_{max} , nm	Lifetime ^a (ns)
L1 (dgpy)	228 (29.0)	311 (12.8)	-----	-----	360	
L2 (dgpz)	224 (26.9)	340 (14.1)	-----	-----	382	
1	218 (64.7)	282 (19.2)	346 (3.5)	-----	381	9.3
2	219 (44.5)	283 (12.4)	318 (7.3)	377 (3.4)	418	11.6
Re(bpy)(py)(CO) ₃ ^b				366 (2.4)	558	658

^adata in dry deareated acetonitrile. ^bfrom ref 6.

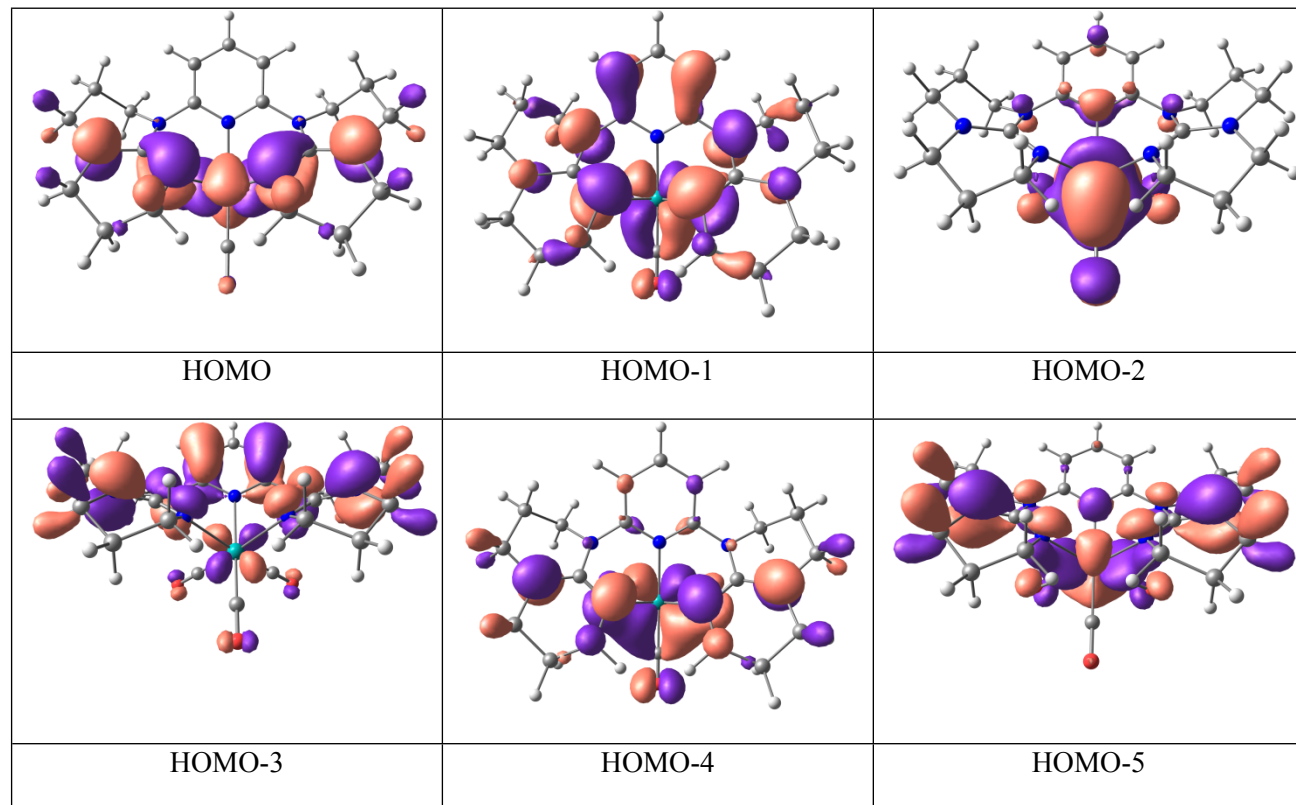
DFT Calculations:

Computational details:

All calculations were performed with the Gaussian03⁷ suite of programs employing the DFT method, the Becke three-parameter hybrid functional,⁸ and Lee-Yang-Parr's gradient-corrected correlation functional (B3LYP).⁹ Singlet ground state geometry optimizations for **1**¹⁺, **2**¹⁺ and **1**²⁺ were carried out at the (R)B3LYP and (U)B3LYP levels, respectively, in the gas phase, using their respective crystallographic structures as starting points. All elements except Re were assigned the 6-31G(d,p) basis set.¹⁰ The double- ζ quality LANL2DZ ECP basis set¹¹ with an effective core potential and one additional f-type polarization was employed for the Re-atom. Vertical electronic excitations based on (R)B3LYP- and (U)B3LYP-optimized geometries were computed for **1**¹⁺, **2**¹⁺ and **1**²⁺, respectively, using the TD-DFT formalism^{12a,b} in acetonitrile using conductor-like polarizable continuum model (CPCM).^{13a-c} Vibrational frequency calculations were performed to ensure that the optimized geometries represent the local minima and there are only positive eigenvalues. The electronic distribution and localization of the singlet excited states were visualized using the electron density difference maps (ED-DMs).¹⁴ *Gausssum* 2.2 and *Chemissian* were employed to visualize the absorption spectra (simulated with Gaussian distribution with a full-width at half maximum (fwhm) set to 3000 cm⁻¹) and to calculate the fractional contributions of various groups to each molecular orbital. All calculated structures and Kohn-Sham orbitals were visualized with ChemCraft.¹⁵

Table S4. MO Composition of $\mathbf{1}^{1+}$ in Singlet ($S=0$) Ground State (b3lyp/LanL2DZ(f)[Re]6-31G**[C,H,N,O]).

MO	Energy (eV)	Composition				
		Re	Py	Hpp	CO (trans to Py)	CO (trans to Hpp)
LUMO+5	-0.04	8	3	69	1	19
LUMO+4	-0.12	0	2	3	25	70
LUMO+3	-0.87	22	9	8	17	43
LUMO+2	-0.91	22	16	5	22	36
LUMO+1	-1.05	2	75	18	2	3
LUMO	-1.70	6	75	8	9	2
HOMO	-5.97	34	0	48	1	17
HOMO-1	-6.14	22	14	55	6	5
HOMO-2	-6.62	61	5	4	13	17
HOMO-3	-6.78	6	31	59	1	2
HOMO-4	-7.05	40	3	40	9	8
HOMO-5	-7.30	23	5	61	0	10



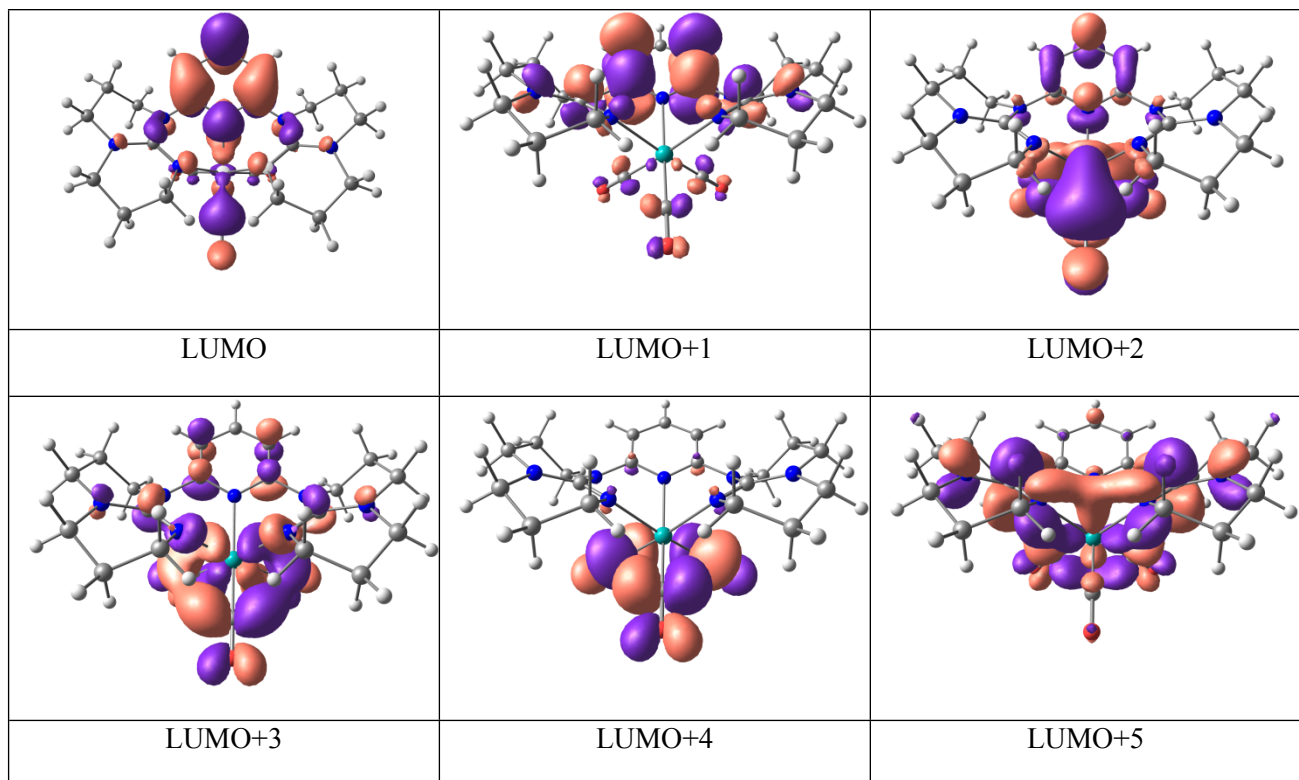


Figure S6. Kohn-Sham molecular orbital diagrams of $\mathbf{1}^{1+}$ in ($S=0$) ground state

Table S5. Selected Transitions from TD-DFT calculations of $\mathbf{1}^{1+}$ in the Singlet Ground State (b3lyp/LanL2DZ(f)[Re]6-31G**[C,H,N,O], CPCM (CH₃CN)).

energy (eV)	λ/nm	$\lambda/\text{nm} (\times 10^3 \text{ M}^{-1}\text{cm}^{-1})$ [expt.]	f	Major transition(s)	character
5.55	223	218 (64.7)	0.1553	H-5 \rightarrow L+1 (33%), H-1 \rightarrow L+7 (26%), H \rightarrow L+6 (16%)	[hpp(n/ π) (major) + Re(d π) (minor) to Py(π^*)] + [hpp(n/ π) (major) + Re(d π) (minor) to hpp(π^*)]
4.39	282	282 (19.2)	0.1143	H-3 \rightarrow L (75%), H \rightarrow L+3 (10%)	hpp(n/ π) (major) + Py(π) (minor) to Py(π^*)
3.61	343	346 (3.5)	0.0199	H-1 \rightarrow L (94%)	hpp(n/ π) (major) + Re(d π) (minor) to Py(π^*)

Table S6. MO composition of $\mathbf{1}^{2+}$ in ($S=1$) ground state in α -spin (ub3lyp/LanL2DZ(f)[Re]6-31G**[C,H,N,O]).

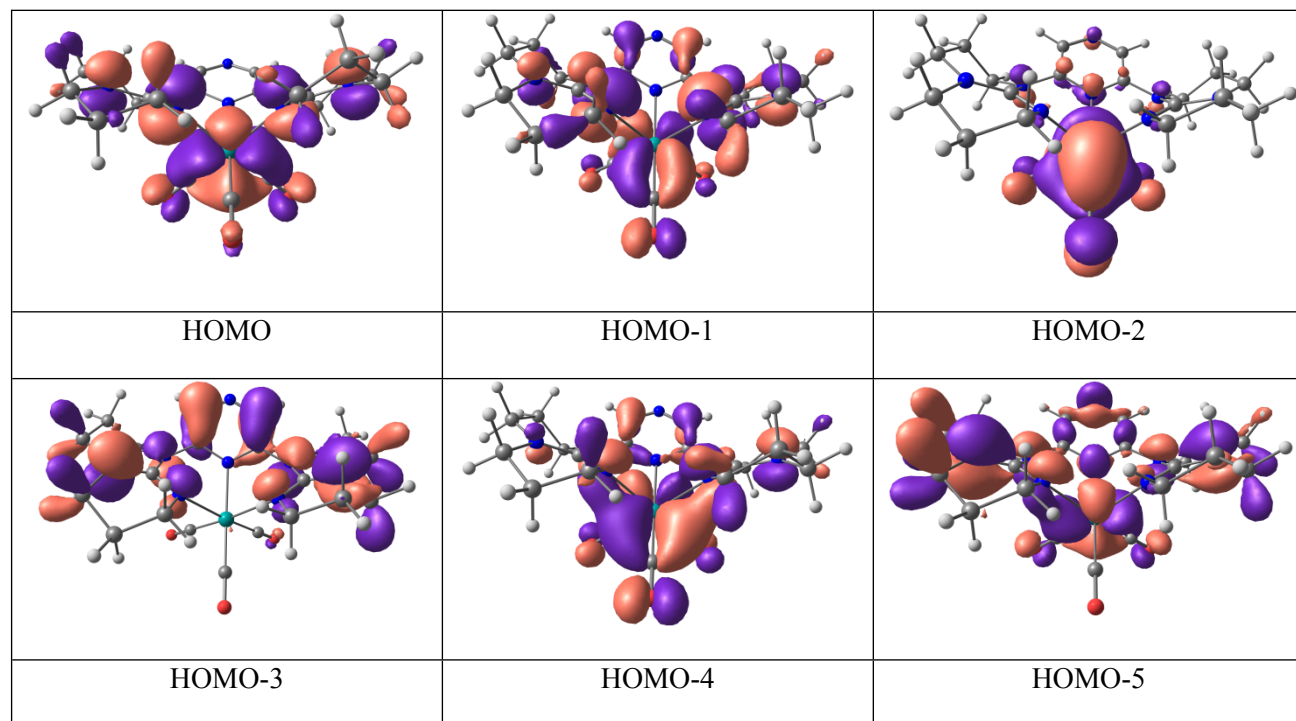
MO	Energy (eV)	Composition				
		Re	Py	Hpp	CO (trans to Py)	CO (trans to Hpp)
LUMO+5	-1.06	1	8	3	15	73
LUMO+4	-1.37	17	3	22	1	57
LUMO+3	-1.55	4	59	10	4	23
LUMO+2	-1.64	14	16	19	13	38
LUMO+1	-1.79	17	25	7	9	42
LUMO	-2.24	10	63	7	14	7
HOMO	-6.84	30	0	56	0	13
HOMO-1	-6.94	16	27	52	3	2
HOMO-2	-7.51	15	22	56	3	4
HOMO-3	-7.66	59	10	8	11	13
HOMO-4	-8.14	9	8	79	0	3
HOMO-5	-8.18	39	4	44	7	5

Table S7. MO composition of $\mathbf{1}^{2+}$ in ($S=1$) ground state in β -spin (ub3lyp/LanL2DZ(f)[Re]6-31G**[C,H,N,O]).

MO	Energy (eV)	Composition				
		Re	Py	Hpp	CO (trans to Py)	CO (trans to Hpp)
LUMO+5	-1.10	16	2	39	0	43
LUMO+4	-1.44	14	22	5	21	38
LUMO+3	-1.57	4	57	22	6	12
LUMO+2	-1.73	17	23	5	13	42
LUMO+1	-2.22	8	66	7	13	6
LUMO	-5.14	38	0	40	0	21
HOMO	-6.73	18	14	61	4	3
HOMO-1	-7.31	3	32	64	0	1
HOMO-2	-7.52	60	8	6	11	14
HOMO-3	-7.90	11	7	77	0	4
HOMO-4	-7.94	50	6	28	10	7
HOMO-5	-8.35	18	9	70	1	2

Table S8. MO Composition of $\mathbf{2}^{1+}$ in Singlet ($S=0$) Ground State (b3lyp/LanL2DZ(f)[Re]6-31G**[C,H,N,O]).

MO	Energy (eV)	Composition				
		Re	Pz	Hpp	CO (trans to Pz)	CO (trans to Hpp)
LUMO+6	+0.11	8	5	70	15	2
LUMO+5	-0.14	11	3	68	0	18
LUMO+4	-0.20	1	1	4	25	69
LUMO+3	-0.97	25	1	10	19	45
LUMO+2	-1.05	26	6	3	26	38
LUMO+1	-1.36	0	84	15	0	1
LUMO	-2.35	3	85	7	4	0
HOMO	-6.06	33	0	50	1	16
HOMO-1	-6.31	24	9	56	6	5
HOMO-2	-6.74	62	4	5	12	17
HOMO-3	-6.91	1	27	71	0	1
HOMO-4	-7.13	43	9	30	9	9
HOMO-5	-7.32	18	14	60	0	8



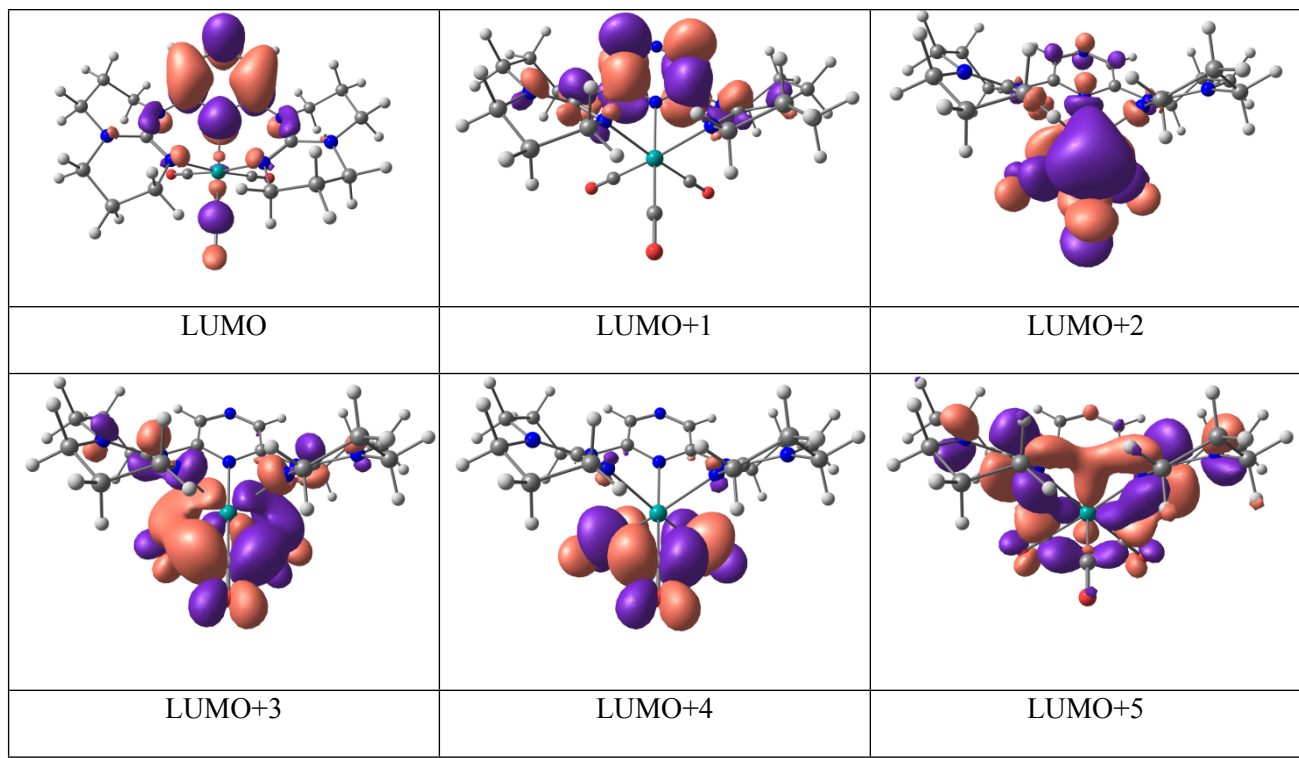


Figure S7. Kohn-Sham molecular orbital diagrams of $\mathbf{2}^{1+}$ in ($S=0$) ground state

Table S9. Selected Transitions from TD-DFT calculations of $\mathbf{2}^{1+}$ in the Singlet Ground State (b3lyp/LanL2DZ(f)[Re]6-31G**[C,H,N,O], CPCM (CH₃CN)).

energy (eV)	λ/nm	$\lambda/\text{nm} (\epsilon \times 10^3 \text{ M}^{-1}\text{cm}^{-1})$ [expt.]	f	Major transition(s)	character
5.42	228	219 (44.5)	0.1714	H -> L+6 (49%)	hpp(n/ π) (major) + Re(d π) (minor) to hpp(π^*)
4.41	281	283 (12.4)	0.0972	H-1 -> L+2 (51%), H -> L+3 (27%)	hpp(n/ π) (major) + Re(d π) (minor) to CO(π^*) (major) + Re(d π^*) (minor)
3.90	318	318 (7.3)	0.0773	H-3 -> L (87%)	hpp(n/ π) (major) + Pz(n/ π) (minor) to Pz(π^*)
3.19	389	377 (3.4)	0.0238	H-1 -> L (96%)	hpp(n/ π) (major) + Re(d π) (minor) to Pz(π^*)

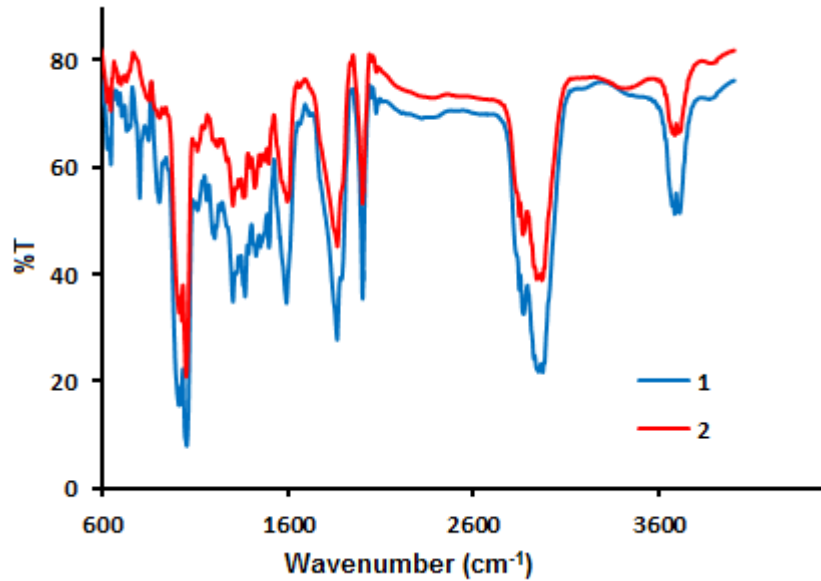


Figure S8. ATR-IR spectra of complexes **1** and **2**, recorded at ambient temperature as solids.

Table S10. Infrared Frequencies: Observed *vs.* Calculated

Compound	Obs. stretching (cm ⁻¹)	Calc. stretching (cm ⁻¹)	Bond involved
1	2003	2093	C20-O1
	1885	2000	C22-O3
	1867	1995	C21-O2
2	2005	2096	C20-O2
	1888	2006	C19-O1
	1868	1999	C21-O3
<i>fac,fac</i> -[Re(bqp - <i>k</i> ³ <i>N</i>)(CO) ₃] ⁺	2028, 1918	-----	-----

bqp = 2,6-bis(8'-quinolinyl)pyridine

Table S11. Electrochemical data of **L1**, **L2**, **1** and **2** and some benchmark complexes.

Compound	$E_{1/2}(\text{ox})^a$			$E_{1/2}(\text{red})^a$		$\Delta E_{1/2}$
L1 (dgpy)	-----	1.11 (308)	0.77 (irr) ^b	-----	-----	-----
L2 (dgpz)	-----	1.14 (189)	0.77 (irr)	-1.99 (irr)	-----	2.76
1	1.43 (100)	1.08 (80)	0.73 (irr) ^b	-1.99 (irr)	-----	2.72
2	1.43 (80)	1.09 (82)	0.72 (irr)	-1.49 (73)	-----	2.22
<i>mer,cis</i> -[Re(tpy- $\kappa^3\text{N}$)(CO) ₂ (P(OEt) ₃)(CF ₃ SO ₃) ^c	1.30 (irr)	0.93 (73)	-----	-1.23 (irr)	-1.5 (irr)	2.16
<i>mer,cis</i> -[Re(tpy- $\kappa^3\text{N}$)(CO) ₂ Cl] ^c	1.22 (irr)	-----	0.48 (65)	-1.17 (irr)	-1.34 (irr)	1.65
[Re(bpy)(CO) ₃ (Py)][ClO ₄] ^d	1.74	-----	-----	-1.09	-1.39	2.83

^aPotentials are in volts vs. SCE in acetonitrile solutions, 0.1 M in [n-Bu₄N]PF₆, recorded at 25 ± 1 °C at a sweep rate as mentioned in experimental section. The difference between cathodic and anodic peak potentials (millivolts) is given in parentheses. ^bIrreversible; potential is given for the anodic wave. ^cFrom ref 5. ^dFrom ref 6.

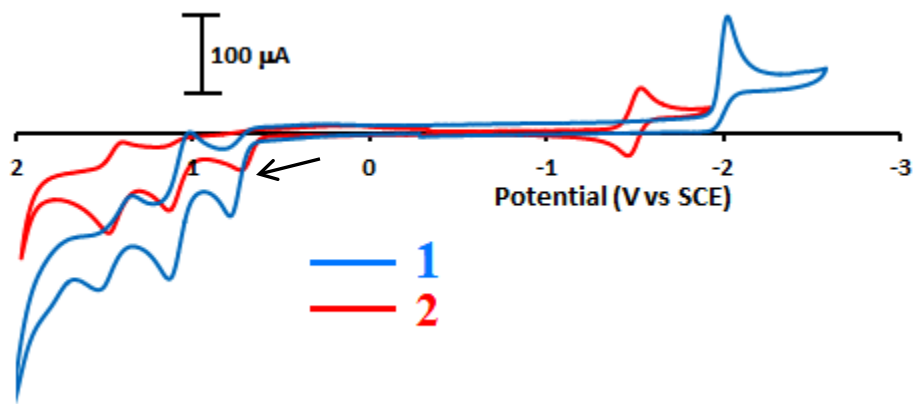


Figure S9. Cyclic voltammogram of complexes **1** and **2** in dry, degassed CH₃CN, recorded at a scan rate of 10 and 25 mV/s, respectively.

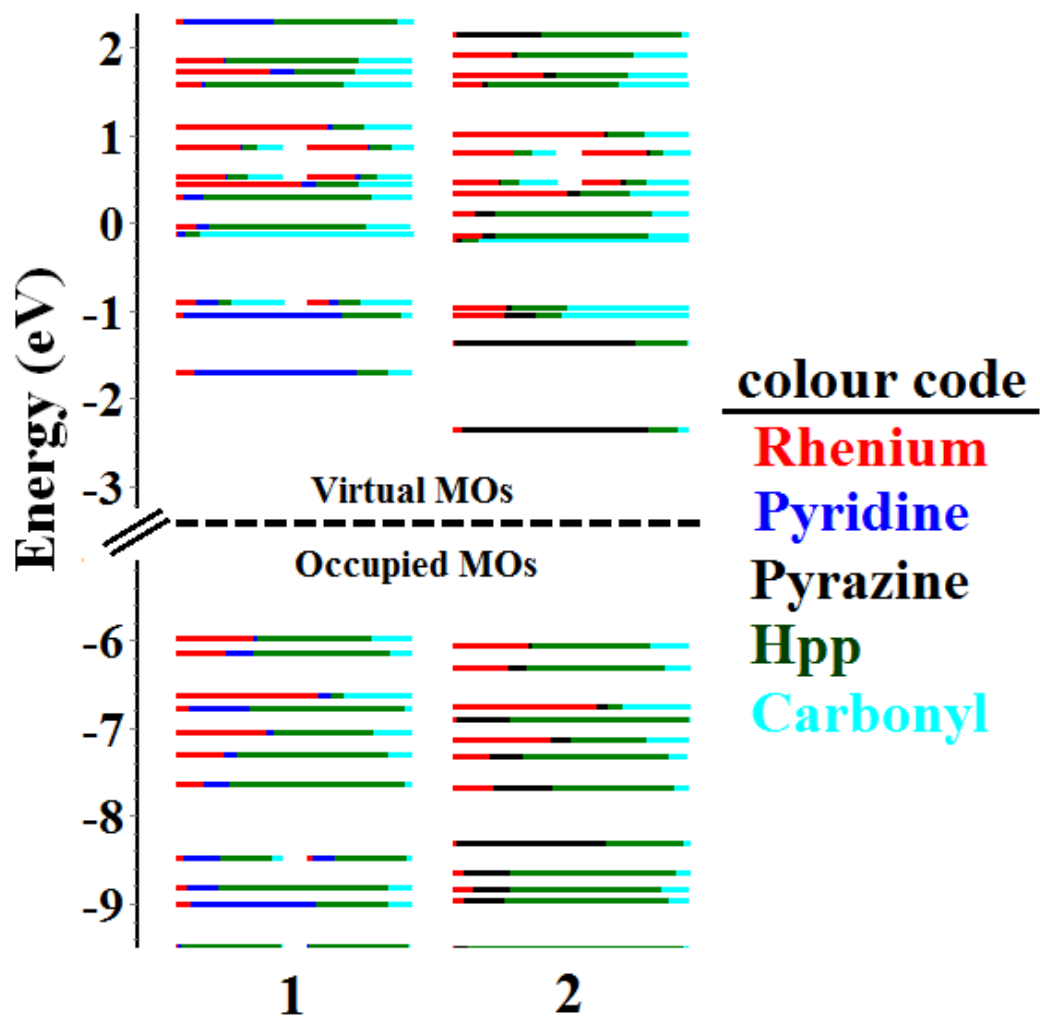


Figure S10. Calculated frontier MO energies of the modeled complexes, **1** and **2** obtained from DFT(b3lyp/LanL2DZ(f)[Re]6-31G**[CHNO] with CPCM(CH₃CN) and 0.05 eV of threshold of degeneracy.

Table S12. Optimized Atomic coordinates obtained from DFT calculations of $\mathbf{1}^{1+}$

Center Number	Atomic Number	Atomic Type	Coordinates (Angstroms)		
			X	Y	Z
1	75	0	-0.000045	-0.766037	0.748959
2	8	0	2.188434	-0.566095	2.920411
3	8	0	-0.000405	-3.842376	1.013527
4	8	0	-2.188380	-0.565700	2.920517
5	7	0	0.000051	1.378688	0.203710
6	7	0	-2.372700	1.310015	0.106480
7	7	0	-3.808899	0.007507	-1.228912
8	7	0	-1.583576	-0.689864	-0.835788
9	7	0	2.372806	1.309799	0.106686
10	7	0	3.808871	0.007474	-1.229120
11	7	0	1.583642	-0.690019	-0.835651
12	6	0	1.171421	2.044684	0.047251
13	6	0	1.200860	3.433053	-0.125057
14	1	0	2.138792	3.956448	-0.246695
15	6	0	0.000183	4.127549	-0.182576
16	1	0	0.000237	5.202897	-0.328043
17	6	0	-1.200557	3.433156	-0.125164
18	1	0	-2.138440	3.956621	-0.246890
19	6	0	-1.171247	2.044787	0.047151
20	6	0	-3.591981	1.971280	0.607391
21	1	0	-3.297707	2.833920	1.203264
22	1	0	-4.096619	1.273049	1.284454
23	6	0	-4.488526	2.329014	-0.571917
24	1	0	-5.393873	2.848361	-0.245068
25	1	0	-3.954986	2.995714	-1.257380
26	6	0	-4.873024	1.026997	-1.267912
27	1	0	-5.749651	0.590708	-0.772516
28	1	0	-5.150706	1.200721	-2.314950
29	6	0	-4.227442	-1.272753	-1.831391
30	1	0	-4.375594	-1.109589	-2.906950
31	1	0	-5.201968	-1.541089	-1.406793
32	6	0	-3.204339	-2.372643	-1.591533
33	1	0	-3.389998	-3.202162	-2.279635
34	1	0	-3.285597	-2.762794	-0.571586
35	6	0	-1.811660	-1.782734	-1.792001
36	1	0	-1.046174	-2.540535	-1.635537
37	1	0	-1.698420	-1.410460	-2.820329
38	6	0	-2.568090	0.164973	-0.688246
39	6	0	3.592088	1.971028	0.607646
40	1	0	4.096694	1.272771	1.284707
41	1	0	3.297812	2.833651	1.203542
42	6	0	4.488673	2.328752	-0.571634
43	1	0	5.393977	2.848187	-0.244803
44	1	0	3.955112	2.995330	-1.257202
45	6	0	4.873277	1.026692	-1.267428
46	1	0	5.151630	1.200360	-2.314293
47	1	0	5.749511	0.590202	-0.771496
48	6	0	4.227259	-1.272631	-1.832038

49	1	0	5.201968	-1.540993	-1.407879
50	1	0	4.374980	-1.109234	-2.907619
51	6	0	3.204332	-2.372635	-1.591994
52	1	0	3.285958	-2.762904	-0.572121
53	1	0	3.389842	-3.202050	-2.280261
54	6	0	1.811532	-1.782848	-1.791953
55	1	0	1.697871	-1.410583	-2.820239
56	1	0	1.046192	-2.540742	-1.635217
57	6	0	2.568162	0.164819	-0.688171
58	6	0	1.363340	-0.652279	2.105257
59	6	0	-0.000239	-2.682021	0.940370
60	6	0	-1.363364	-0.652046	2.105299

Table S13. Optimized Atomic coordinates obtained from DFT calculations of **2¹⁺**

Center Number	Atomic Number	Atomic Type	Coordinates (Angstroms)		
			X	Y	Z
1	75	0	0.013673	-0.781041	0.765764
2	8	0	2.208585	-0.519033	2.924365
3	8	0	0.096155	-3.857669	1.046418
4	8	0	-2.171290	-0.642276	2.945522
5	7	0	-0.046399	1.346319	0.218823
6	7	0	-0.144445	4.082819	-0.260951
7	7	0	-2.417824	1.237299	0.161365
8	7	0	-3.847517	-0.079514	-1.170717
9	7	0	-1.605078	-0.741036	-0.797316
10	7	0	2.325374	1.390874	0.073640
11	7	0	3.821388	0.088320	-1.189715
12	7	0	1.613223	-0.669826	-0.808140
13	6	0	1.090000	2.052573	0.016700
14	6	0	1.016599	3.437656	-0.206297
15	1	0	1.911068	4.029168	-0.365182
16	6	0	-1.259096	3.367299	-0.147574
17	1	0	-2.197402	3.900145	-0.255242
18	6	0	-1.233113	1.980606	0.068206
19	6	0	-3.624040	1.867339	0.734740
20	1	0	-3.318771	2.759290	1.280660
21	1	0	-4.045558	1.172361	1.470187
22	6	0	-4.623193	2.160088	-0.375805
23	1	0	-4.180180	2.845793	-1.105987
24	1	0	-5.526276	2.634742	0.018213
25	6	0	-4.993555	0.836615	-1.034718
26	1	0	-5.758484	0.324627	-0.435609
27	1	0	-5.419224	1.001961	-2.030683
28	6	0	-4.135024	-1.350955	-1.851121
29	1	0	-5.019820	-1.200018	-2.473637
30	1	0	-4.375362	-2.127471	-1.112258
31	6	0	-2.925807	-1.743631	-2.688464
32	1	0	-3.095007	-2.702359	-3.187105

33	1	0	-2.767451	-0.989075	-3.466964
34	6	0	-1.711602	-1.842393	-1.769686
35	1	0	-1.745336	-2.784636	-1.209270
36	1	0	-0.793484	-1.857611	-2.362819
37	6	0	-2.607203	0.090178	-0.636864
38	6	0	3.512283	2.134285	0.541743
39	1	0	4.045725	1.497041	1.255900
40	1	0	3.175792	3.013269	1.089441
41	6	0	4.392846	2.469258	-0.655082
42	1	0	5.270596	3.049368	-0.356832
43	1	0	3.828712	3.070944	-1.375418
44	6	0	4.841876	1.149961	-1.275313
45	1	0	5.121886	1.278010	-2.328100
46	1	0	5.730644	0.780119	-0.748951
47	6	0	4.301609	-1.204010	-1.717617
48	1	0	5.272605	-1.415143	-1.254489
49	1	0	4.473726	-1.086845	-2.795376
50	6	0	3.310660	-2.326668	-1.451067
51	1	0	3.378611	-2.667821	-0.412792
52	1	0	3.540598	-3.179620	-2.095691
53	6	0	1.905176	-1.793574	-1.712645
54	1	0	1.812506	-1.465950	-2.758315
55	1	0	1.160502	-2.569919	-1.545686
56	6	0	2.568128	0.222340	-0.675118
57	6	0	1.381640	-0.630186	2.115261
58	6	0	0.063254	-2.699652	0.962882
59	6	0	-1.348895	-0.705005	2.126232

Table S14. Optimized Atomic coordinates obtained from DFT calculations of **1²⁺**

Center Number	Atomic Number	Atomic Type	Coordinates (Angstroms)		
			X	Y	Z
1	75	0	0.000040	-0.752473	0.611551
2	8	0	2.125759	-0.644050	2.922570
3	8	0	0.000862	-3.849575	0.733280
4	8	0	-2.126213	-0.647389	2.922326
5	7	0	-0.000065	1.402992	0.172189
6	7	0	-2.382587	1.352153	0.134703
7	7	0	-3.879488	-0.015253	-1.048082
8	7	0	-1.629965	-0.687304	-0.777073
9	7	0	2.382509	1.352464	0.134198
10	7	0	3.879493	-0.015420	-1.047867
11	7	0	1.629936	-0.687329	-0.776938
12	6	0	1.169860	2.069616	-0.005655
13	6	0	1.199125	3.439677	-0.274172
14	1	0	2.138323	3.953878	-0.423977
15	6	0	-0.000266	4.129789	-0.389954

16	1	0	-0.000343	5.191035	-0.615832
17	6	0	-1.199561	3.439592	-0.273742
18	1	0	-2.138851	3.953730	-0.423178
19	6	0	-1.170106	2.069508	-0.005333
20	6	0	-3.572506	2.062675	0.665937
21	1	0	-3.234938	2.962662	1.176283
22	1	0	-4.032459	1.418096	1.423172
23	6	0	-4.543614	2.337788	-0.473670
24	1	0	-5.427083	2.875611	-0.119651
25	1	0	-4.066457	2.957349	-1.239813
26	6	0	-4.969381	0.992501	-1.046210
27	1	0	-5.784132	0.567796	-0.449167
28	1	0	-5.333531	1.086192	-2.074848
29	6	0	-4.328077	-1.321901	-1.591383
30	1	0	-4.559870	-1.169213	-2.651867
31	1	0	-5.262700	-1.582368	-1.084672
32	6	0	-3.276415	-2.404291	-1.415561
33	1	0	-3.493088	-3.236310	-2.090633
34	1	0	-3.283835	-2.799462	-0.394252
35	6	0	-1.915868	-1.789870	-1.719639
36	1	0	-1.119436	-2.527259	-1.645511
37	1	0	-1.892610	-1.391549	-2.743397
38	6	0	-2.628405	0.191656	-0.599519
39	6	0	3.572396	2.063188	0.665266
40	1	0	4.032306	1.418875	1.422755
41	1	0	3.234807	2.963356	1.175265
42	6	0	4.543536	2.337870	-0.474418
43	1	0	5.426969	2.875886	-0.120609
44	1	0	4.066353	2.957081	-1.240830
45	6	0	4.969377	0.992356	-1.046362
46	1	0	5.333577	1.085605	-2.075022
47	1	0	5.784100	0.567920	-0.449091
48	6	0	4.328240	-1.322404	-1.590281
49	1	0	5.262447	-1.582819	-1.082772
50	1	0	4.560849	-1.170156	-2.650646
51	6	0	3.276262	-2.404567	-1.414834
52	1	0	3.283151	-2.799695	-0.393505
53	1	0	3.493033	-3.236673	-2.089767
54	6	0	1.915980	-1.789847	-1.719511
55	1	0	1.893333	-1.391358	-2.743219
56	1	0	1.119325	-2.527037	-1.645887
57	6	0	2.628388	0.191740	-0.599524
58	6	0	1.359842	-0.690854	2.069056
59	6	0	0.000508	-2.697175	0.707369
60	6	0	-1.360037	-0.692673	2.068973

References:

1. (a) S. P. Schmidt, W. C. Trogler, F. Basolo, *Inorg. Syn.*, 1990, **28**, 154; (b) A. K. Pal, N. Zaccheroni, S. Campagna, G. S. Hanan, *Chem. Commun.*, 2014, accepted for publication.
2. *APEX2 (2007) version 2.4-0; Bruker Molecular Analysis Research Tool.* Bruker AXS Inc., Madison, WI 53719-1173.
3. Sheldrick, G. M. (1996). *SADABS*, Bruker Area Detector Absorption Corrections. Bruker AXS Inc., Madison, WI 53719-1173.
4. *SHELXTL (2001) version 6.12;* Bruker Analytical X-ray Systems Inc., Madison, WI 53719-1173.
5. (a) Losey, D. J.; Frenzel, B. A.; Smith, W. M.; Hightower, S. E.; Hamaker, C. G. *Inorg. Chem. Commun.* **2013**, *30*, 46. (b) Frenzel, B. A.; Schumaker, J. E.; Black, D. R.; Hightower, S. E. *Dalton Trans.* **2013**, *42*, 12440.
6. L. A. Sacksteder, A. P. Zipp, E. A. Brown, J. Streich, J. N. Demas, B. A. DeGraff, *Inorg. Chem.*, 1990, **29**, 4335.
7. M. J. Frisch, G. W. Trucks, H. B. Schlegel, G. E. Scuseria, M. A. Robb, J. R. Cheeseman, J. A. Montgomery, T. J. Vreven, K. N. Kudin, J. C. Burant, J. M. S. Millam, J. Tomasi, V. Barone, B. Mennucci, M. Cossi, G. Scalmani, N. Rega, G. A. Petersson, H. Nakatsuji, M. Hada, M. Ehara, K. Toyota, R. Fukuda, J. Hasegawa, M. Ishida, T. Nakajima, Y. Honda, O. Kitao, H. Nakai, M. Klene, X. Li, J. E. Knox, H. P. Hratchian, J. B. Cross, C. Adamo, J. Jaramillo, R. Gomperts, R. E. Startmann, O. Yazyev, A. J. Austin, R. Cammi, C. Pomelli, J. W. Ochterski, P. Y. Ayala, K. Morokuma, G. A. Voth, P. Salvador, J. J. Dannenberg, V. G. Zakrzewski, J. M. Dapprich, A. D. Daniels, M. C. Strain, O. Farkas, D. K. Malick, A. D. Rabuck, K. Raghavachari, J. B. Foresman, J. V. Ortiz, Q. Cui, A. G. Baboul, S. Clifford, J. B. Cioslowski, G. Liu, A. Liashenko, I. Piskorz, L. M. R. Komaromi, D. J. Fox, T. Keith, M. A. Al-Laham, C. Y. Peng, A. Manayakkara, M. Challacombe, P. M. W. Gill, B. G. Johnson, W. Chen, M. W. Wong, C. Gonzalez, J. A. Pople, *Gaussian 2003, Revision C.02; Gaussian Inc.:Pittsburgh PA, 2003.*

8. A. D. Becke, *J. Chem. Phys.*, 1993, **98**, 5648.
9. C. Lee, W. Yang, R. G. Parr, *Phys. Rev. B: Condens. Matter*, 1988, **37**, 785.
10. A. D. McLean, G. S. Chandler, *J. Chem. Phys.*, 1980, **72**, 5639.
11. P. J. Hay, W. R. Wadt, *J. Chem. Phys.*, 1985, **82**, 270.
12. (a) M. E. Casida, C. Jamorski, K. C. Casida, D. R. Salahub, *J. Chem. Phys.*, 1998, **108**, 4439; (b) R. E. Stratmann, G. E. Scuseria, M. J. Frisch, *J. Chem. Phys.*, 1998, **109**, 8218.
13. (a) M. Cossi, N. Rega, G. Scalmani, V. Barone, *J. Comput. Chem.*, 2003, **24**, 669; (b) M. Cossi, V. Barone, *J. Chem. Phys.*, 2001, **115**, 4708; (c) V. Barone, M. Cossi, *J. Phys. Chem. A*, 1998, **102**, 1995.
14. W. R. Browne, N. M. O'Boyle, J. J. McGarvey, J. G. Vos, *Chem. Soc. Rev.*, 2005, **34**, 641.
15. D. A. Zhurko, G. A. Zhurko, *ChemCraft 1.5*; Plimus: San Diego, CA. Available at <http://www.chemcraftprog.com>.